Coherent Amplification of an Ultrashort Pulse in a High- and Swept-Gain Medium with Level Degeneracy

Chul Min Kim and Jongmin Lee*
Center for Femto-Atto Science and Technology, and Advanced Photonics Research Institute, Gwangju Institute of Science and Technology, Gwangju 500-712, Korea

Karol A. Janulewicz†
School of Photon Science and Technology, Gwangju Institute of Science and Technology, Gwangju 500-712, Korea
(Received 16 October 2009; published 4 February 2010)

A one-dimensional model of the coherent amplification in a high- and swept-gain amplifier in the presence of strong spontaneous emission is presented and applied to seeding an x-ray laser with a high harmonic pulse. The atomic structure of the amplifying medium includes level degeneracy, and the Maxwell-Bloch equations are used to describe the propagation and interaction processes. This analysis elucidates, in the most comprehensive way, the influence of the random spontaneous emission on the coherent amplification process, as reflected in the basic pulse parameters such as its shape, polarization, and coherence.

DOI: 10.1103/PhysRevLett.104.053901 PACS numbers: 42.55.Vc, 42.50.Md, 42.65.Ky

Seeding of a high-gain medium by injecting an ultrashort coherent pulse is a rare realization of the coherent amplification process—a fundamental phenomenon in the laser physics and spectroscopy. In this regime of amplification, the pulse duration of the seed is shorter than or comparable to the dipole relaxation time of the medium. The nonadiabatic variation of the electric dipole induced by the external radiation becomes crucial, and, instead of the rate equations, the Maxwell-Bloch equations for the complex envelopes of the physical quantities should be employed without any adiabatic approximations [1]. Moreover, the high gain reinforces the influence of the spontaneous noise on the coherent amplification of the seed. This influence is most likely reflected in the phase-related properties like polarization, coherence, and divergence.

This basic process of coherent amplification obtained practical attention when the development towards an ultimate short-wavelength source began. Both the laser-plasma-based and free-electron x-ray lasers (XRLs) have shown some disadvantages in their natural working regimes of amplified spontaneous emission (ASE) or self-amplified spontaneous emission (SASE), respectively. The "quantum" (laser-plasma-based) XRL has a low level of spatial coherence and random polarization while the free-electron XRL has limited temporal coherence. There has been much effort in developing the seeding technique to overcome these disadvantages and obtain more stable and better defined parameters [2–6]. The seed pulse should have favorable properties such as short pulse duration, well-defined polarization, superb spatial coherence, and low divergence. When such a pulse is injected into an active medium, the amplified output pulse may inherit the good properties of the seed.

Recently, several theoretical works applying the Maxwell-Bloch equations to describe the seeding effect were reported [7–9]. In these analyses, the atomic level degeneracy was not treated properly, and the important radiation parameters depending on phase, e.g., polarization, could not be discussed. To investigate these properties, a thorough consideration of the level degeneracy is required. This can be demonstrated with the simplest degenerate lasing system in Fig. 1(a), where the Λ-type (two-level but three-state) system in Ag^{19+} is schematically depicted [10]. The selection rules require that the transition on the left-hand side ($m = 0 \leftrightarrow m = -1$) involves only the left- circularly polarized radiation while the other transition ($m = 0 \leftrightarrow m = 1$) is permitted only for the right-circularly polarized light [11]. When the incident pulse is polarized along the x axis, the coherent interaction leads to a coherent combination of the two transitions with effective polarization along the x axis. Clearly, such a system can be simplified to a two-state atomic structure. However, in an active medium with high gain, the strong

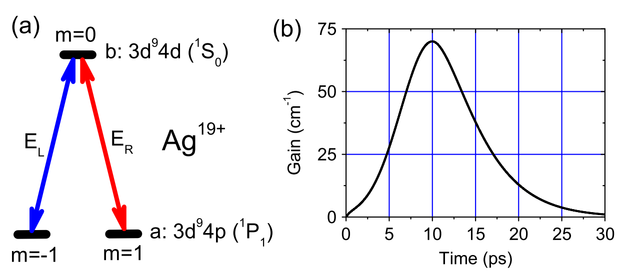

FIG. 1 (color online). (a) Atomic energy levels involving the lasing transitions and (b) time-dependant gain of the medium; the gain peak of 70 cm^{-1} is at 10 ps, and the gain duration (FWHM) is 9.8 ps. Although the lower level has a state with $m = 0$ (not shown here), the transition $m = 0 \leftrightarrow m = 0$ does not contribute to the stimulated emission along the pulse propagation direction (the z axis).

spontaneous noise being the source of ASE is randomly polarized, and it competes with the seed pulse in the amplification process. In such a case, the two transitions involving the different states of the lower laser level should be treated as separate ones [12].

In the present Letter, we investigate the propagation of an ultrashort seed pulse in an active medium by using the numerical solution of the Maxwell-Bloch equations with fully incorporated level degeneracy and in the presence of the high level ASE—the combination that may reveal the competitiveness of random spontaneous emission and coherent seed in the most comprehensive way but has not been considered yet. The time-dependent pumping and relaxation are included in these equations [9]. The lasing transition $4d(^1S_0) \rightarrow 4p(^1P_1)$ at 13.9 nm in nickel-like silver (Ag^{19+}) and a high harmonic (HH) seed have been chosen for modeling because it fulfils all requirements for the coherent amplification mentioned above, and reliable experimental data are available [5]. Not only the temporal pulse shape and energy amplification but also polarization and correlation of the field components are discussed by considering the pulse structure.

For the sake of simplicity, the seed pulse is injected into a uniform high- and swept-gain amplifier. One-dimensional propagation along the z axis is assumed. A beam cross section area of 400 μm^2 has been chosen close to that in the experiment. The time-dependent gain of the medium is shown in Fig. 1(b). The atomic states are denoted by b, a, and the value of m (± 1); the circular polarization states are denoted by L and R. In the moving frame ($\tau = t - z/c$), the core of the Maxwell-Bloch equation set written in atomic units is as follows [12].

$$\partial N_b/\partial\tau = -\gamma_b N_b + \mathrm{Im}\{P_R E_R^* + P_L E_L^*\}/2 + R_b$$
$$\partial N_{a1}/\partial\tau = -\gamma_a N_{a1} + \mathrm{Im}\{P_R^* E_R\}/2 + \gamma_{\mathrm{bir}} N_b$$
$$\partial P_R/\partial\tau = -\gamma_{ba1} P_R + \Gamma_R - i z_{ba}^2\{E_R(N_b - N_{a1}) + n_i \rho_{-1,1} E_L\}$$
$$\partial(n_i\rho_{1,-1})/\partial\tau = -\gamma_{1,-1} n_i \rho_{1,-1} + i\{P_R^* E_L - P_L E_R^*\}/4$$
$$\partial E_R/\partial z = (i2\pi\omega_0/c)(P_R - n_e E_R/\omega_0^2),$$

N and $\rho_{1,-1}$ are the population and the density matrix element involving the lower states, respectively. P and E are the complex amplitudes obtained from the analytic signals [13] of the induced macroscopic dipole and the electric field, respectively. The remaining equations for $N_{a,-1}$, P_L, and E_L are obtained from the equations presented above by performing the subscript exchanges $1 \leftrightarrow -1$ and $R \leftrightarrow L$. $R_b(\tau)$ is the pumping term, and $\Gamma_{L \text{ or } R}(N_b, \tau)$ are the random sources representing spontaneous emission [14]. The values of numerical parameters are as follows: resonant energy $\hbar\omega_0 = 89.2$ eV ($\lambda_0 = 13.9$ nm); population relaxation constants $\gamma_a = 2.33$ THz and $\gamma_b = 2.56$ THz; electron density $n_e = 2.0 \times 10^{20}$ cm^{-3}, ion density $n_i = 9.1 \times 10^{15}$ cm^{-3}; radiative relaxation constant $\gamma_{\mathrm{bir}} = 0.059$ THz; dipole relaxation constants $\gamma_{ba} = 3.39$ THz and $\gamma_{1,-1} = 3.27$ THz; and dipole matrix element $z_{ba} = 0.274$. These values were obtained from atomic structure calculation [15], laser-plasma simulation [16], and experimental report on linewidth measurement [17]. The equations were solved self-consistently, and the Runge-Kutta 4th order algorithm accompanied by a statistical method for dealing with random function [18] were used.

The temporal shape of the output pulse from the seeded active medium develops a unique structure, as shown in Fig. 2. The pulse shape was obtained by summing the instantaneous values of $|E_L|^2$ and $|E_R|^2$. The ultrashort HH pulse (25 fs, 1 nJ, polarized along the x axis) is injected into the medium at the moment of gain peak (10 ps), as the plot at 0 mm shows. Because the intensity of the seed pulse is much higher than that of spontaneous emission (SE), the medium is put immediately in a coherent state, which is followed by emission of a coherent echo owing to the free induction decay (the plot at 1 mm). This echo is amplified in propagation and develops an oscillating and then decaying pulse shape (the plots at 2 mm and 3 mm), the signature of Rabi oscillation and polarization decay. The polarization components of this part of radiation are expected to be strongly correlated, and the effective field is polarized along the x axis as the seed pulse. In further propagation, the randomly polarized ASE grows in front of the coherent part (the plots at 4 mm and 5 mm). Consequently, the output pulse consists of two distinct parts: i.e., the ASE with random polarization and the amplified seed assumed to have the polarization of the input pulse. The width of the main spike in the output pulse is 170 fs (FWHM), and its intensity is larger than that of the ASE by almost an order of magnitude.

The full incorporation of the level degeneracy enabled an explicit examination of the polarization state. The inset in Fig. 2 shows the temporal variation of the y component of the electric field with respect to the x component within the duration of the output pulse at 5 mm medium length.

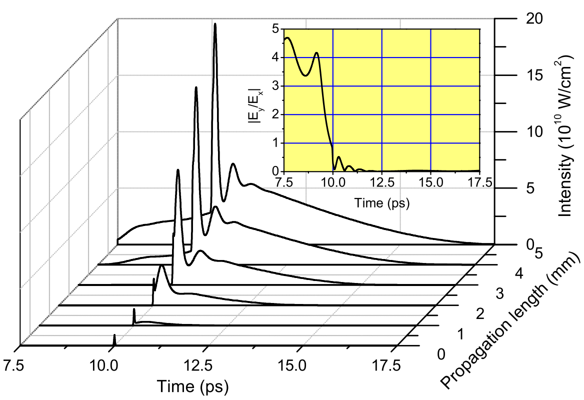

FIG. 2 (color online). Evolution of the seed pulse as it propagates through the lasing medium. The duration (FWHM) of the main peak at 5 mm is 170 fs. The inset shows the relative magnitude of the y component of the electric field with respect to the x component ($|E_y/E_x|$) at 5 mm.

Within the ASE, $|E_y|$ can be even larger than $|E_x|$ because ASE is randomly polarized. Emission by the induced dipole in this part will reproduce the ASE polarization feature. After the ASE component has passed, the dipole interacts with the coherent part polarized along the x axis, and the dipole starts to adjust itself to the polarization direction of the driving field, i.e., to the x axis. The resultant radiation during the adjustment shows $|E_y|$ decreasing towards 0 in an oscillatory way.

This specific pulse structure consisting of the prepulse ASE followed by the coherent seeded part leads to the pulse characteristics which are dramatically different from those of the conventional ASE-XRLs. Figure 3 presents the pulse energy dependence on the length of the amplifying medium and its second-order derivative with respect to the propagation length. The maximum of the second-order derivative gives the curvature transition point that can be treated as the beginning of saturation and called the saturation point [19]. Unlike the ASE-XRLs, the seeded XRL has two saturation points at 1.0 mm and at 3.6 mm. To identify the origin of each saturation point, either the random source or the seed was neglected in the equations. It was found that the first point at 1.0 mm corresponds to the seeded component, and the next one at 3.2 mm to ASE. Saturation of the coherent component appears first because the seed pulse is much stronger than the SE starting at the amplifier entrance and dominates the interaction in early propagation stages.

Such a pulse structure also has important implication on the polarization of the output radiation. Figure 4 shows the dependence of the degree of polarization (DOP) on the propagation length for seeding in the presence of SE, seeding in the absence of SE, and pure ASE. Seeding together with SE gives a DOP very close to 1.0 (reproducing the linear polarization of the seed) over the propagation distance up to 3 mm. After that, the ASE signal begins to be comparable to the coherent part, and the DOP starts to be reduced. This reduction is attributed to the influence of the noticeable ASE signal.

DOP lowering with the increase in the ASE signal has two facets. The DOP of a pure ASE is lower than that of a pure coherent echo due to the stochastic nature of the SE, as shown in Fig. 4. Consequently, the increased contribution of the ASE component reduces the DOP calculated from the whole pulse. In addition, the preceding ASE component degrades the following coherent part in the way described above; the low-level oscillation of $|E_y/E_x|$ in the inset of Fig. 2 is the signature of the depolarization in the coherent part.

From the results given above, it is concluded that the ASE level should be kept as low as possible to obtain well-defined polarization of the output pulse reproducing that of the seed. To achieve this, the medium length has to be limited (here 3 mm). In this case, however, the pulse energy is significantly reduced from 1007 nJ to 311 nJ, as shown in Fig. 3. A better solution is to adjust the injection time of the seed pulse to make the coherent part the dominating one. In the previous considerations, the seed pulse was incident at the moment of maximum gain (10 ps). Figure 5 shows the variation of the energy and DOP with the adjustment of the injection time for a 5-mm medium. When the injection time is 7 ps, i.e., 3 ps before the gain peak, the DOP is kept nearly 1.0. Moreover, the energy has the maximum value of 1127 nJ, exceeding that obtained without adjusting the injection time. With this optimum value of the injection time, energy extraction from the lasing medium is mostly through coherent interaction. Consequently, the polarization of the seed pulse is mostly conserved. When the injection is either too early (earlier than 4 ps) or too late (later than 16 ps), the ASE becomes dominant over the coherent part because the latter is ineffectively induced in the small gain areas. In these cases, the energy and DOP have values close to those of the ASE-XRLs.

When the numerical results obtained above are compared with the experimental results, the one-dimensional nature of the model should be taken into account; the

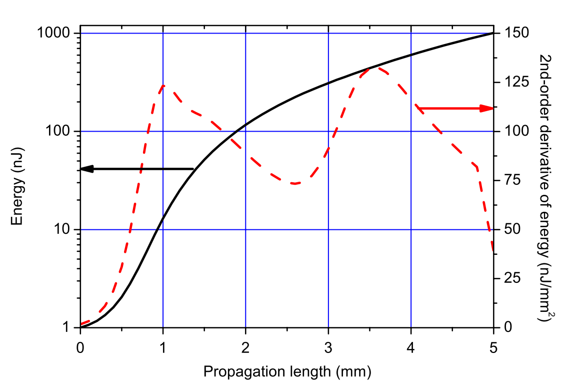

FIG. 3 (color online). Pulse energy (solid line) and 2nd-order derivative of the pulse energy (with respect to the propagation length) (dashed line) as a function of propagation length. The values were obtained by averaging over 24 different realizations of random number sequences.

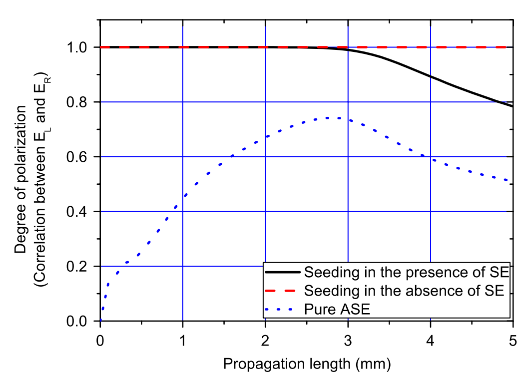

FIG. 4 (color online). Degree of polarization (or correlation between E_L and E_R) as a function of propagation length for seeding in the presence of spontaneous emission (SE) (solid line), seeding in the absence of SE (dashed line), and pure ASE (dotted line). The values were obtained by averaging over 24 different realizations of random number sequences.

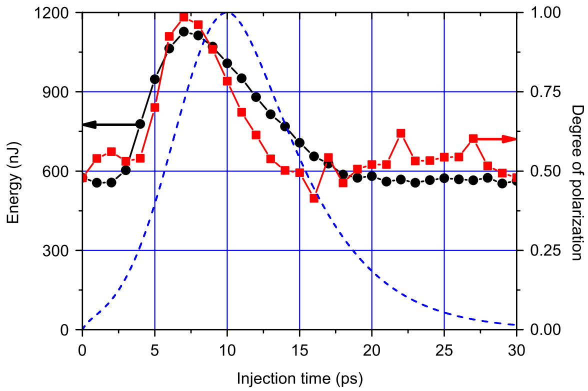

FIG. 5 (color online). Pulse energy (circle) and degree of polarization (square) at 5 mm as a function of the seed injection time. The normalized gain (dashed line) is also shown. The values were obtained by averaging over 24 different realizations of random number sequences.

numerical results can be considered to pertain to a single ray. In the experimental conditions, the inhomogeneity of the active medium modifies the features observed above. For example, the characteristic pulse structure may be smeared due to the overlapping of the differently delayed or bent rays, and the DOP of ASE may be reduced further because the SE sources have no spatial correlation. Moreover, other properties like spatial coherence and divergence cannot be investigated properly with the current one-dimensional model in principle. In spite of this, the improvement of these properties is expected because the coherent parts of the bunch of rays are induced by the same seed pulse, and it may increase the spatial correlation along transverse directions. The improvement of spatial coherence and divergence was experimentally observed [5].

In conclusion, we have numerically investigated various output pulse characteristics such as pulse shape, energy, and DOP. They were explained by considering the pulse structure consisting of the randomly polarized ASE and the coherent part well reproducing the polarization of the seeding pulse. It was found that the ASE component of the output pulse obstructs the inheritance of the superb phase properties of the input seeding pulse. These observations provide important implications both for the fundamental physics of laser amplifiers and for the experimental realization of an x-ray/extreme ultraviolet (XUV) source with outstanding properties. The characteristic features presented above are expected to be present over a broad range of gain values because they depend mostly on the predominance of the HH intensity over the ASE intensity, which is the usual case in the experiments. As the gain increases (decreases), all the dynamics features are observed within a shorter (longer) medium.

The energy extraction of the seeded high-gain medium (XRL) is not very much improved in comparison to that of the conventional ASE-XRLs—it is just doubled. However, due to the spike formed at the beginning of the coherent part, the intensity can be enhanced by an order of magnitude, and the pulse duration as short as 170 fs can be obtained. To conserve the linear polarization, excellent spatial coherence, and low divergence of the seed, the ASE level should be reduced, e.g., by adjusting injection time of the seed. To realize the initial dream of a mJ short-wavelength source with good properties [4], a very long amplifier or multiple amplifying stages might be necessary. In such a case, the deteriorating effect of ASE will be eventually unavoidable even if the injection time is adjusted. Injection of multiple seed pulses may mitigate this problem because the coherent interaction may be adjusted to prevail over the whole gain duration.

We thank P. V. Nickles for the important comments on the manuscript. This work was supported by the Ministry of Knowledge and Economy of Korea through the Ultrashort Quantum Beam Facility Program and also partially by the Basic Science Research Program through the National Research Foundation of Korea (NRF) funded by the Ministry of Education, Science and Technology (No. R15-2008-006-03001-0).

*leejm@gist.ac.kr
†kaj@gist.ac.kr

[1] F. A. Hopf and M. O. Scully, Phys. Rev. **179**, 399 (1969).
[2] J. Costello, Nat. Photon. **2**, 67 (2008).
[3] T. Ditmire *et al.*, Phys. Rev. A **51**, R4337 (1995).
[4] Ph. Zeitoun *et al.*, Nature (London) **431**, 426 (2004).
[5] Y. Wang *et al.*, Nat. Photon. **2**, 94 (2008).
[6] G. Lambert *et al.*, Nature Phys. **4**, 296 (2008).
[7] I. R. Al'miev *et al.*, Phys. Rev. Lett. **99**, 123902 (2007).
[8] B. Robillart *et al.*, in *X-Ray Lasers 2008, Proceedings of the 11th International Conference on X-Ray Lasers, Belfast, UK*, edited by C. L. S. Lewis and D. Riley (Springer, Dordrecht, 2009).
[9] C. M. Kim, K. A. Janulewicz, H. T. Kim, and J. Lee, Phys. Rev. A **80**, 053811 (2009).
[10] N. Hasegawa *et al.*, J. Opt. Soc. Korea **13**, 60 (2009).
[11] A. Sureau and P. B. Holden, Phys. Rev. A **52**, 3110 (1995).
[12] B. W. Shore, *The Theory of Coherent Atomic Excitation* (Wiley, New York, 1990).
[13] M. Born and E. Wolf, *Principles of Optics* (Cambridge University Press, Cambridge, 2005), 7th ed.
[14] O. Larroche *et al.*, Phys. Rev. A **62**, 043815 (2000).
[15] MCDFGME (MultiConfiguration Dirac Fock and General Matrix Elements program, release 2005) edited by J. P. Desclaux and P. Indelicato (http://dirac.spectro.jussieu.fr/mcdf).
[16] G. J. Pert, J. Fluid Mech. **131**, 401 (1983).
[17] P. Jaeglé, *Coherent Sources of XUV Radiation: Soft X-Ray Lasers and High-Order Harmonic Generation* (Springer, New York, 2005).
[18] S. Chandrasekhar, Rev. Mod. Phys. **21**, 383 (1949).
[19] C. Imesch *et al.*, in *X-Ray Lasers 2008, Proceedings of the 11th International Conference on X-Ray Lasers, Belfast, UK*, edited by C. L. S. Lewis and D. Riley (Springer, Dordrecht, 2009).